Title

Assessment of Porcine Intervertebral Disc Specimen pH via Chemical Exchange Saturation Transfer (CEST) MRI

Permalink

https://escholarship.org/uc/item/0hm3j31w

Author

Grabau, Michelle Annette

Publication Date

2012

Peer reviewed|Thesis/dissertation

ASSESSMENT OF PORCINE INTERVERTEBRAL DISC SPECIMEN PH VIA CHEMICAL EXCHANGE SATURATION TRANSFER (CEST) MRI

By

Michelle Grabau

Submitted in partial satisfaction of the requirements for the degree of

MASTER OF SCIENCE

In

Biomedical Imaging

in the

GRADUATE DIVISION

of the

UNIVERSITY OF CALIFORNIA, SAN FRANCISCO

Dedications and Acknowledgements

First, I would like to thank my family, in particular my fantastic parents Susan and Michael,

and loved ones for always supporting me in everything I do including all academic ventures.

I would also like to thank Dr. Gerd Melkus and Dr. Sharmila Majumdar for their continuous

support and ongoing mentoring throughout this entire process.

Assessment of Porcine Intervertebral Disc Specimen pH via Chemical Exchange Saturation Transfer (CEST) MRI

Michelle Grabau

Abstract

Low back pain is an expensive, widespread healthcare concern. The mechanisms of its progression and association with intervertebral disc degeneration are not fully understood, but recent studies suggest that lactate accumulation and a subsequent drop in pH may be initiating events. Chemical exchange saturation transfer (CEST) of glycosaminoglycans (gagCEST) has emerged as way to quantify glycosaminoglycan (GAG) concentrations in the intervertebral disc, but no studies have examined its dependency on pH. This study seeks to assess the pH-dependence of gagCEST and use iopromide, a common contrast agent used in CT imaging, as a pH-sensitive CEST probe to explore these agents' potential to measure pH of the intervertebral discs. We first create chondroitin sulfate and Ultravist® phantoms over a range of pH values to explore the pH-dependency of the CEST imaging of these probes and apply these findings to porcine intervertebral disc specimens. Our results demonstrate the non-linear dependence of gagCEST on pH and a linear regression of the Iopromide CEST effect with pH ($R^2 = 0.95$). Iopromide was then infused into the disc and the calibration created by the phantom studies was used to determine pH in the disc.

These findings provide what is to our knowledge the first description of the pH dependence of gagCEST imaging and the first use of the iopromide contrast agent in the CEST MR imaging of the intervertebral disc specimen. Because iopromide CEST imaging is independent of the local concentration of macromolecules, it particularly shows great potential in reporting pH in intervertebral disc specimen studies. The

ability to report pH in a tissue non-invasively by one of these methods could be valuable

in better understanding disease progression.

Table of Contents

Introduction

Low back pain (LBP) is a major health concern, resulting in nearly 15 billion dollars of healthcare and other costs to society in the United States yearly [1]. Intervertebral disc degeneration (IVD) is considered one of the underlying factors of LBP [2] and is defined as an 'aberrant, cell-mediated response to progressive structure failure' [3]. However, degenerative discs can be asymptomatic suggesting that degeneration itself may not be sufficient to cause back pain [4]. The pathophysiology and progression of discogenic back pain remain unclear.

Physiology and Biochemistry of the Intervertebral Disc

The intervertebral disc lies between the bony vertebral bodies of the spinal column. Its main purpose is to transmit loads through the spinal column and resist spinal compression while maintaining flexibility to allow for bending, flexing, and rotation. The intervertebral disc consists of distinct tissue components including the annulus fibrosis, the outer cartilaginous ring that maintains the flexibility of the spinal column, and the nucleus pulposus, a gelatinous core that prevents the annulus from buckling under pressure and thus provides the resistive properties of the disc. The nucleus pulposus is comprised largely of proteoglycans, molecules with a protein core with multiple chains of glycosaminoglycans (GAG's) covalently attached. The GAG's are long, unbranched carbohydrates of repeating disaccharide units [5]. Aggrecan, the main proteoglycan found in the disc, consists of the GAG's keratin sulfate and chondroitin sulfate, two highly anionic molecules that provide the osmotic properties that keep the disc hydrated.

Under healthy conditions, the matrix of the disc is a dynamic structure with a delicate balance of matrix degradation and synthesis regulated by the cells of the disc.

1

The disc is highly avascular and thus nutrients must diffuse significant distances (up to 5 mm) from nearby, peripheral capillaries. The disc cells are consequently metabolically challenged and rely largely on anaerobic glycolysis to generate energy and lactic acid is produced at high rates [6]. Because metabolic by-products must also diffuse across large distances, lactic acid and other wastes tend to accumulate in the disc. Normally, low concentrations of these wastes help maintain an equilibrium disc pH of 7.2 to 7.7 [7]. However, under high loads or at other times where the cells of the disc may be metabolically taxed, lactate may accumulate in the center of the disc. The subsequent drop in pH (to <6.8) has been shown to cause a number of metabolic changes to the cells of the disc: an up-regulation in the production of extracellular matrix (ECM) degradation enzymes and a down-regulation in the production of ECM constituents (i.e. proteoglycans) and may contribute to disc degeneration [8].

Studies have linked low pH and loss of GAG concentrations in patients with discogenic back pain [9]. One possible explanation for the pain is the disc degeneration that occurs as a result of the metabolic changes that occur with a drop in pH. Another hypothesis, however, is low pH and the subsequent up-regulation of pro-inflammatory cytokines promote nerve ingrowth into the disc, in particular those types of neurons that mediate pain [10]. The presence of these nerves continues to cause excess inflammation response and perpetually destroy the delicate nutrient-metabolite balance of the disc. The biochemical changes such as decrease in pH are therefore crucial components of detecting and understanding intervertebral disc degeneration and chronic back pain.

Imaging the Intervertebral Disc

Magnetic resonance imaging (MRI), as well as computed tomography (CT) and radiographs, have been used to assess IVD anatomy and disc degeneration [11]. These methods, however, offer only structural information with disc morphology qualitatively

assessed using established grading schemes. Furthermore, morphological changes are not well correlated with discogenic pain [12]. Proteoglycans and pH may be the biomarkers needed for the quantification of back pain and disease [9]. One possible method of quantitatively describing GAG or metabolite concentrations within the disc is chemical exchange saturation transfer (CEST) MRI.

CEST magnetic resonance imaging has recently emerged as an alternative source of contrast to the conventional T_1 and T_2 weighted sequences in which contrast can be generated "at will" depending on the either endogenous or exogenous agent selected [13]. CEST imaging is based on the phenomenon of "magnetization transfer," first described by Dr. Bob Balaban *et al* [14]. Magnetization transfer occurs between two pools of protons in chemical exchange, usually labile protons from immobilized macromolecules or exogenous molecules and bulk water. CEST contrast is observed in a decrease in the bulk water signal by frequency selective saturation of labile protons (like on –NH or –OH groups) exchanging with the bulk water protons [15]. Because labile protons all resonate at characteristic frequencies and because solute protons can belong to either endogenous or exogenous "agents," CEST imaging is very versatile imaging technique that has been used to probe pH, temperature, enzyme or macromolecule concentration, and gene activity [13].

CEST agents are classified as either DIACEST (diamagnetic agents) or PARACEST (paramagnetic agents) depending on the magnetic properties of the probe. Many CEST agents have small frequency offset values corresponding with protons from hydroxyl (-OH) or amine (-NH) groups. With ample hydroxyl and amine groups, glycosaminoglycans (GAG's) make excellent DIACEST agents and the relationship between glycosaminoglycan chemical exchange saturation transfer (gagCEST) and GAG concentration in the intervertebral disc has been well-established [16]. The protonation

of these groups is sensitive to changes in pH, but there have been no studies that examine the effect of changing pH on gagCEST signal.

While GAG's are an example of a potential endogenous CEST probe, exogenous contrast agents can also be used. For example, iopromide, a common contrast agent used in CT-protocol, has been successfully used as a multi-contrast agent in MRI [17]. The iopromide molecule consists of two amide groups that generate different CEST effects, resonating at distinct frequencies of 4.2 and 5.6 ppm greater than bulk water resonance. The ratio of these CEST effects is correlated with pH. This method has recently been used to measure pH in *in vivo* tumor models but has not, to our knowledge, been implemented in other tissue types [18].

Purpose

Changes in pH can affect the exchange rate of labile protons with bulk water, making CEST agents pH-responsive probes [15]. Because the accumulation of lactate and the subsequent decrease in pH seem to be an initiating steps in disc degeneration and discogenic back pain, a non-invasive method to measure pH in the disc using pH-responsive CEST probes would be valuable in both research and clinical settings. The purpose of this study is to characterize and assess the pH-dependence of CEST MR imaging in chondroitin sulfate and iopromide phantoms and apply these findings to porcine intervertebral disc specimens.

Materials and Methods

Phantom and Specimen Preparation

A chondroitin sulfate solution (Sigma-Aldrich, St. Louis, MO) was diluted with H_2O to 200 mM and separated into 8 tubes. Samples were titrated with NaOH and/or

HCl to obtain a range of pH values: 5.66, 5.96, 6.10, 6.49, 6.76, 7.07, 7.5, and 7.86. Ultravist® 370 (Bayer Healthcare Pharmaceuticals, 1 mL contains 0.769 g of iopromide) was also diluted in H_2O to 200 mM, separated into 7 additional tubes and titrated to a range of pH values: 5.96, 6.18, 6.40, 6.70, 6.88, 7.12, and 7.48. The pH of each individual sample was measured using a pH meter (Oakton ION 510 series, Vernon Hills, IL).

All of the porcine lumbar spine samples were obtained from a U.S. Department of Agriculture-approved slaughterhouse (Baigio Artisan Meats, Oakland CA) 5-6 hours after slaughter (2- to 5- month-old piglets) and were frozen at -80°C until used. After thawing, the soft tissue was removed first. The samples were cut such that the discs were completely separated from the vertebral bone with all other anatomical regions of the disc in tact. After baseline imaging, discs were injected with 1M lactate solution and imaged using the same parameters. Discs were then dissected in order to measure the pH of the nucleus pulposus. The pH of the disc was proofed using a tissue pH meter (Oakton ION 510 Series, Vernon Hills, IL) as well as pH indicator paper (Merck KGaA, Darmstadt, Germany).

MRI Experiments

All imaging was done on a 7 Tesla (310 mm bore size) superconducting magnet equipped with actively shielded imaging gradients (400 mT/m maximum gradient strength, 120 mm inner bore size) (Agilent Technologies, Palo Alto, CA, USA). A 38 mm inner diameter quadrature ^{1}H birdcage resonator (Agilent Technologies, Palo Alto, CA, USA) was used for RF pulse transmission and signal reception. After checking the position of the phantom by acquiring scout images, the main magnetic field B_0 was shimmed using a global 3D field mapping sequence. CEST experiments were done on the phantoms to optimize the pre-saturation length and RF power of the CEST sequence

and to create the pH calibration curves for both the chondroitin sulfate and Ultravist®

phantoms.

Three MR experiments were then done on the discs. The first was a double

quantum filtered lactate editing spectroscopic imaging sequence (TR = 1s, TE = 144 ms,

FOV = 40 x 40 mm, Matrix = 16x16, slice thickness = 3.8mm, bandwidth = 6 kHz,

spectral points = 256, total time = 8min 32s [19]). $T_{1\rho}$ imaging was accomplished with a

$T_{1\rho}$ preparation module combined with a 3D gradient echo imaging readout module

(MAPSS sequence [20]). For every $T_{1\rho}$ preparation field cycling was used to compensate

for T_1 relaxation effects. TR = 8 ms, TE = 3.5 ms, views per segment = 64, TRseg = 1718

ms, α = 8°, BW = 35.7 kHz, FOV = 40x40x16 mm3, matrix = 192x128x12, resolution =

0.208 x 0.312 x 1.333 mm3, global pre-saturation (three sinc pulses, t_P = 1 ms, α = 90°),

relaxation delay = 1.2 s. 12 different spin lock times (TSL = 0, 1, 2, 5, 8, 10, 20, 40, 60,

100, 200, 300 ms) were used using a spin lock frequency of B_1 = 2 kHz to acquire data

for the $T_{1\rho}$ map. The total scan time for the $T_{1\rho}$ experiment was 16 min 30s.

For CEST imaging, a pulsed CEST-preparation module was used with a single

slice turbo spin echo (TSE) imaging sequence (slice thickness = 6 mm, field of view = 40

x 40 mm, imaging matrix = 64 x 64, echo train length (ETL) = 32, TR = 3000 ms, TEeff

= 35.5 ms). gagCEST z-spectra of the chondroitin sulfate phantoms and intervertebral

discs were acquired using 30 pre-saturation Gaussian pulses with a pulse bandwidth =

25 Hz (FWHM) and a RF pulse power of B_1 = 0.075 µT over a bandwidth of −1 kHz to +1

kHz around the water resonance in 25 Hz steps. Iopromide CEST z-spectra of the

Ultravist® phantoms and intervertebral discs infused with Ultravist® were acquired

using 30 pre-saturation Gaussian pulses with pulse bandwidth = 50 Hz (FWHM) and a

RF pulse power of B_1 = 0.1 µT over a bandwidth of − 3 kHz to +3 kHz around the water

resonance in 50 Hz steps. For each study, one dataset was acquired with limited RF

power (B_1=0.02 μT, number pulses=10) for WASSR field correction [21]. Additionally, one dataset was acquired with the RF pulse was turned off for reference ($CEST_{off}$).

Data Processing

Lactate Maps

The raw lactate spectroscopic imaging datasets were zero filled by a factor of four in the spatial dimensions before Fourier transformation. Lactate maps were created by integrating the Lac CH_3 resonance at 1.3 ppm.

$T_{1\rho}$ Data Processing

The raw 3D $T_{1\rho}$ datasets were zero filled by a factor two in every dimension before Fourier transformation. The $T_{1\rho}$ datasets at different SL frequencies were fitted pixel by pixel to an exponential signal decay model M = M_0·exp(-TSL/$T_{1\rho}$) using a in-house written c-routine.

CEST Processing

The raw data was loaded into MATLAB and the images acquired at the different frequency offsets were reconstructed into a 3D volume. On a pixel-by-pixel basis, CEST raw data was corrected for using the WASSR correction method detailed by Kim, *et al* [21]. Z-spectra were interpolated using a spline interpolation and CEST asymmetry maps were created by subtraction of the signal from the positive frequency offset from the negative. This difference was then divided by the $CEST_{off}$ dataset. These were displayed for the phantoms as well as the discs.

pH dependence of gagCEST was researched using the z-spectra of the chondroitin sulfate phantoms. ROI's were manually drawn in each of the phantoms and the z-spectra in each ROI were averaged. Asymmetry curves were created for each of the phantoms and the integral of the curves from 0.5 to 1.5 ppm, the frequency offset of the

–OH groups in gagCEST [16], as well as the percent asymmetry at 0.75 ppm were calculated. The data plotted against the known pH of the samples to obtain the gagCEST pH-dependency curves. To calibrate the pH-dependence of iopromide CEST, the peaks of the CEST-resonances of the amide groups at 4.2 and 5.6 ppm were measured and the ratio [amplitude of peak at 4.2 ppm / amplitude of peak at 5.6 ppm] calculated. The log of this ratio was plotted against the known pH of the sample.
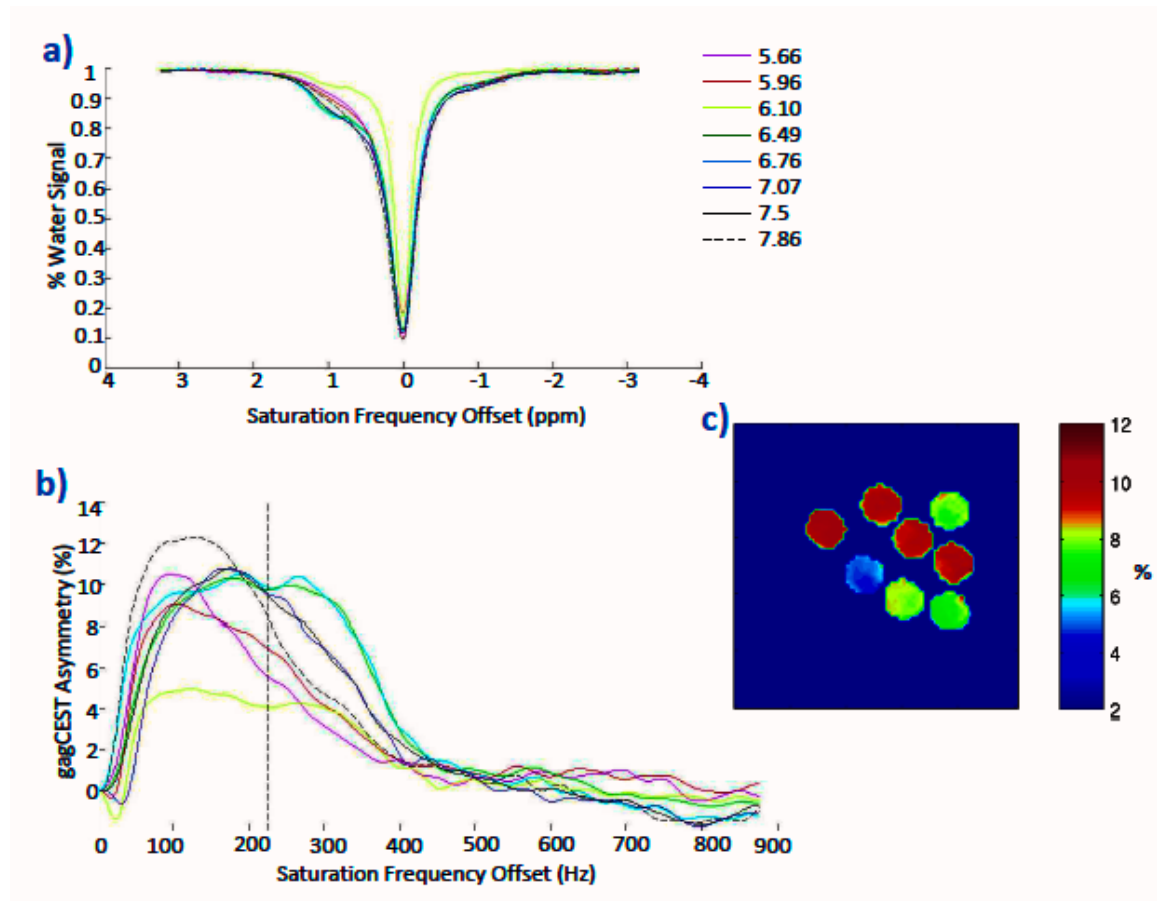
Results

gagCEST Studies

The z-spectra of 200 mM chondroitin sulfate phantoms at varying pH's (Figure 1a) demonstrate that the CEST effect of the –OH groups from 0.5 ppm to 2 ppm from the bulk water resonance varies with pH. This variation is better visualized in the z-spectral asymmetry plots (Figure 1b) and the asymmetry map (Figure 1c). In general, the asymmetry curves of the low pH phantoms show a sharp peak centered at 0.5 ppm, which becomes broader and flatter with a center around 0.6 ppm in the mid-range pH values and then returns at pH > 7.5. The integrals in this range of the asymmetry plots and % asymmetry at 0.75 ppm were found in MATLAB and are shown in Table 1.

| pH	Area from 0.5 - 1.5 ppm	% Asymmetry at 0.75 ppm
5.66	11.23	5.57
5.95	13.45	6.93
6.1	9.60	4.08
6.49	22.53	9.73
6.76	22.87	9.84
7.07	19.41	9.56
7.5	19.40	9.46
7.86	16.32	8.44

Table 1: gagCEST phantom results

The phantom with a pH = 6.10 is an outlier: the CEST effect was much less in this

8

phantom than in the other phantoms. pH-dependency curves were created by plotting the results from the CEST asymmetry analysis against pH. Both the integral from 0.5 to 1.5 ppm and the percent asymmetry at 0.75 ppm increase with increasing pH until pH ≈ 6 to 6.5 and then level and slightly decrease again. This reflects a non-linear change with pH (Figures 1d and 1e).
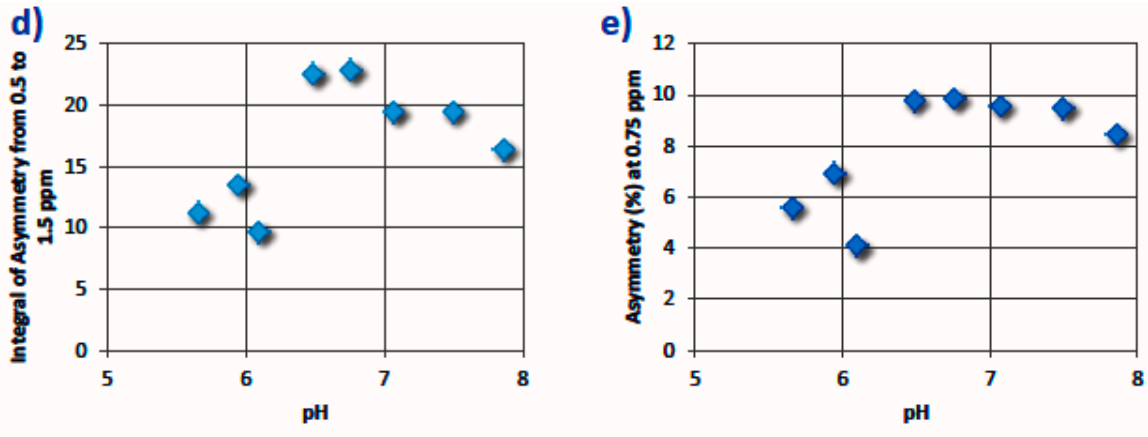
**Figure 1: Chondroitin Sulfate Phantom Results**

(a) Z-spectra of the 8 phantoms (200 mM, varying pH) and the associated asymmetry plots (b) with 0.75 ppm gagCEST denoted as a dashed line. (c) Asymmetry map of the phantoms. Integral of asymmetry plot from 0.5 to 1.5 ppm (d) and % asymmetry at 0.75 ppm (e) as a function of pH.

Five discs were imaged at baseline after deicing. After this baseline imaging, discs were removed from the scanner and injected with 1M lactate solution. The discs were then dried and returned to the scanner for follow-up MR experiments. Special care was taken to ensure that discs were positioned within the coil in the same configuration as at baseline. Lactate spectroscopic imaging was done pre- and post- lactate injection to ensure that the lactate solution was successfully incorporated into the disc. Lac images from Disc 1 are shown below and are representative of the results obtained from all 5 discs. Lactate imaging shows an 10-fold increase in the lactate signal amplitude post-injection, demonstrating that lactate was indeed incorporated into the disc (Figure 2a). $T_{1\rho}$ values increased in all 5 discs after lactate injection, with mean values of 242.4 ms pre-lactate and 382.6 ms post-lactate injection (Figure 2b). These results are consistent with adding fluid to the sample.

CEST results from Disc 5 are shown below and are representative of results from all discs. The asymmetry maps (Figures 2c) and z-spectra asymmetry plots (Figures 2d and 2e) show that the gagCEST signal increases post-lactate injection. Because of the

non-linear relationship between pH and gagCEST signal, no pH change prediction is given for the disc with and without lactate.

d)

e)
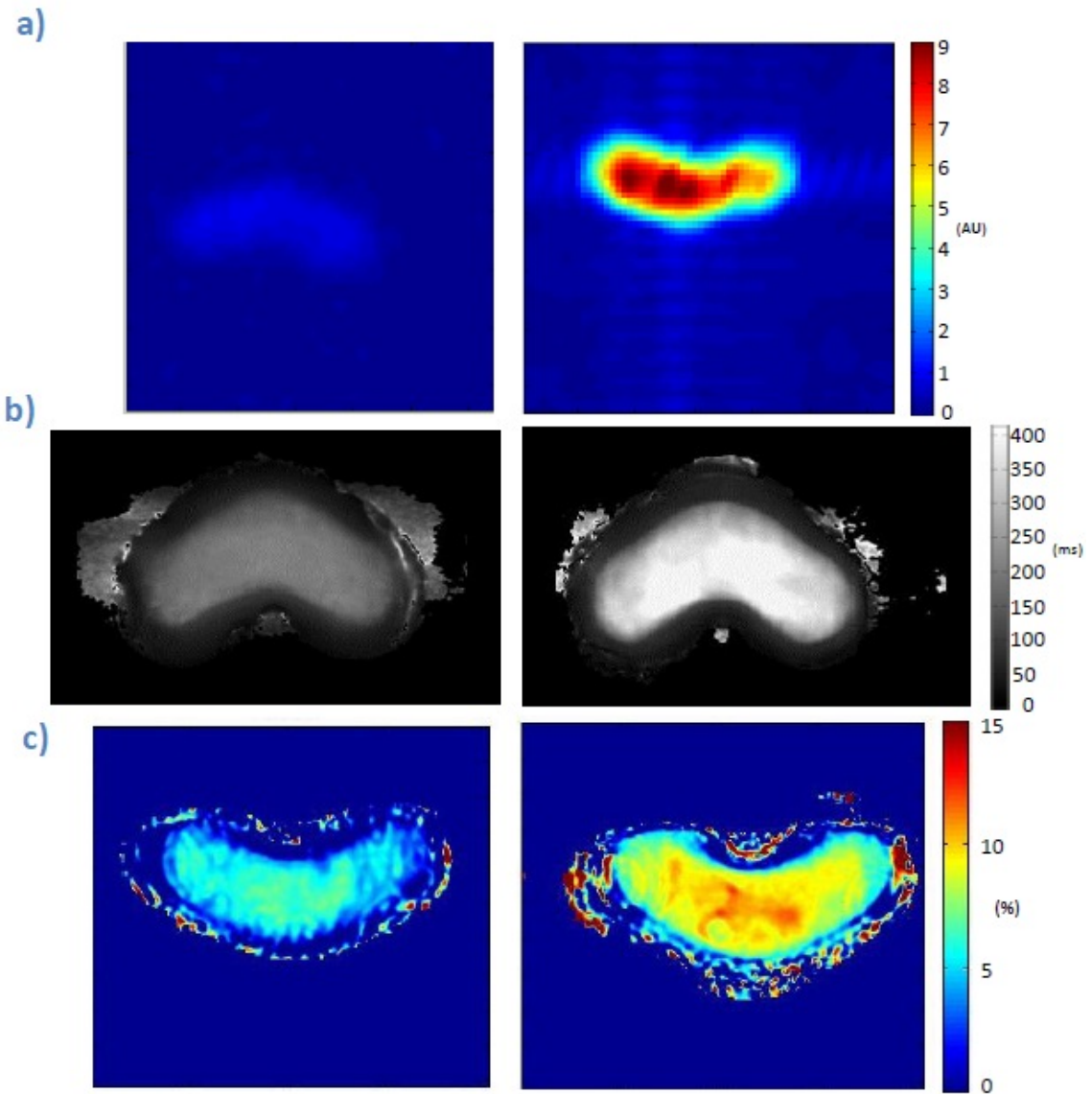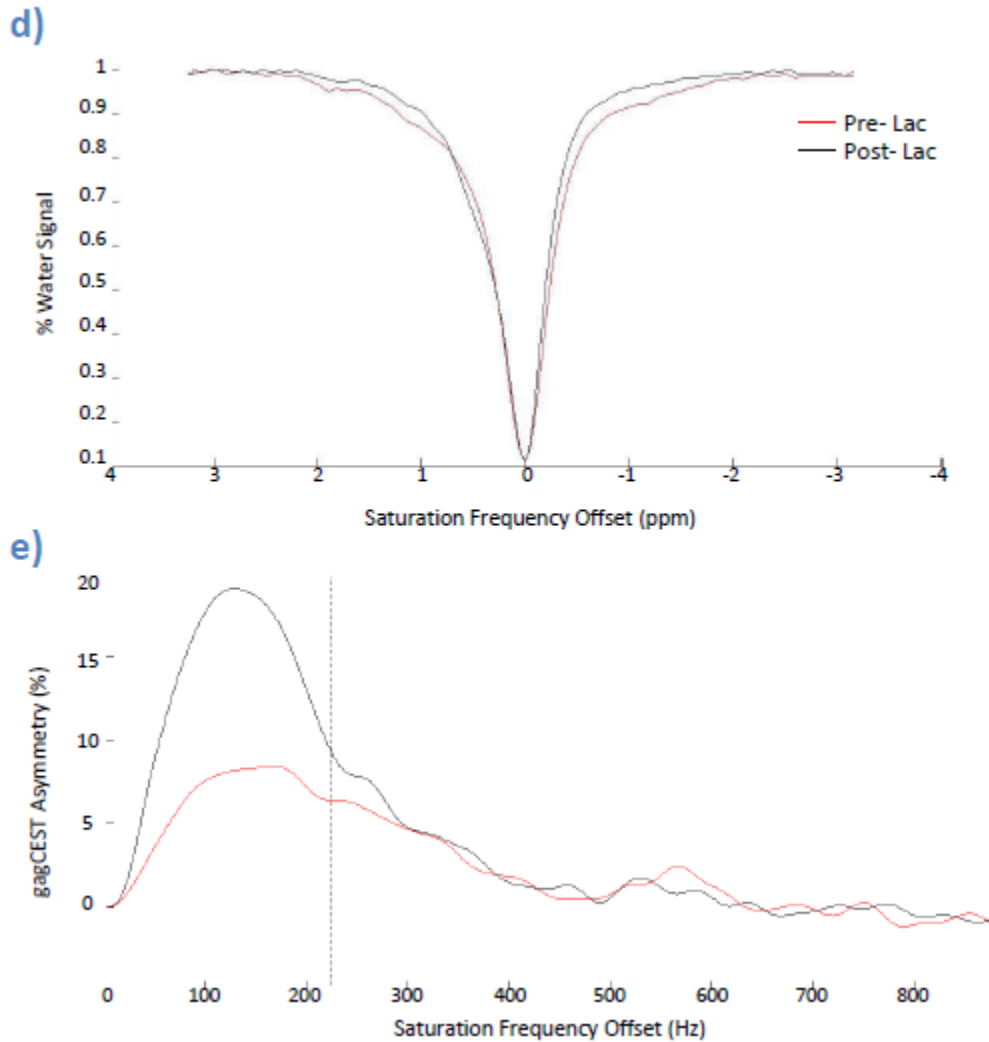
Figure 2: gagCEST Disc Results

Lactate maps (a) show a nearly 10x signal amplitude in disc post-lactate injection and $T_{1\rho}$ – weighted images show greater signal in discs post-lactate (b). Asymmetry maps (c) show greater gagCEST asymmetry in discs injected with lactate, and z-spectra (d) and asymmetry plots (e) confirm the changing gagCEST effect after addition of the acid (shown in black).

Iopromide CEST Studies

The z-spectra of the 200 mM Ultravist® phantoms at varying pH's (Figure 3a) demonstrate a change in the CEST effect of the ratio of the peaks at 4.2 and 5.6 ppm. At low pH, the peak centered at 5.6 ppm is sharp and much more prominent than the peak at 4.2 ppm, with about a 10% decrease in water signal occurring at 5.6 ppm. With increasing pH, the peak at 5.6 ppm flattens and then nearly disappears at pH's > 7.12,

12

while the peak at 4.2 ppm consistently becomes sharper. The ratios of the two peaks [amplitude of peak at 4.2 ppm / amplitude of peak at 5.6 ppm] were calculated and plotted with respect to pH fitting a linear regression trend with an R^2 of 0.95 (Figure 3b).
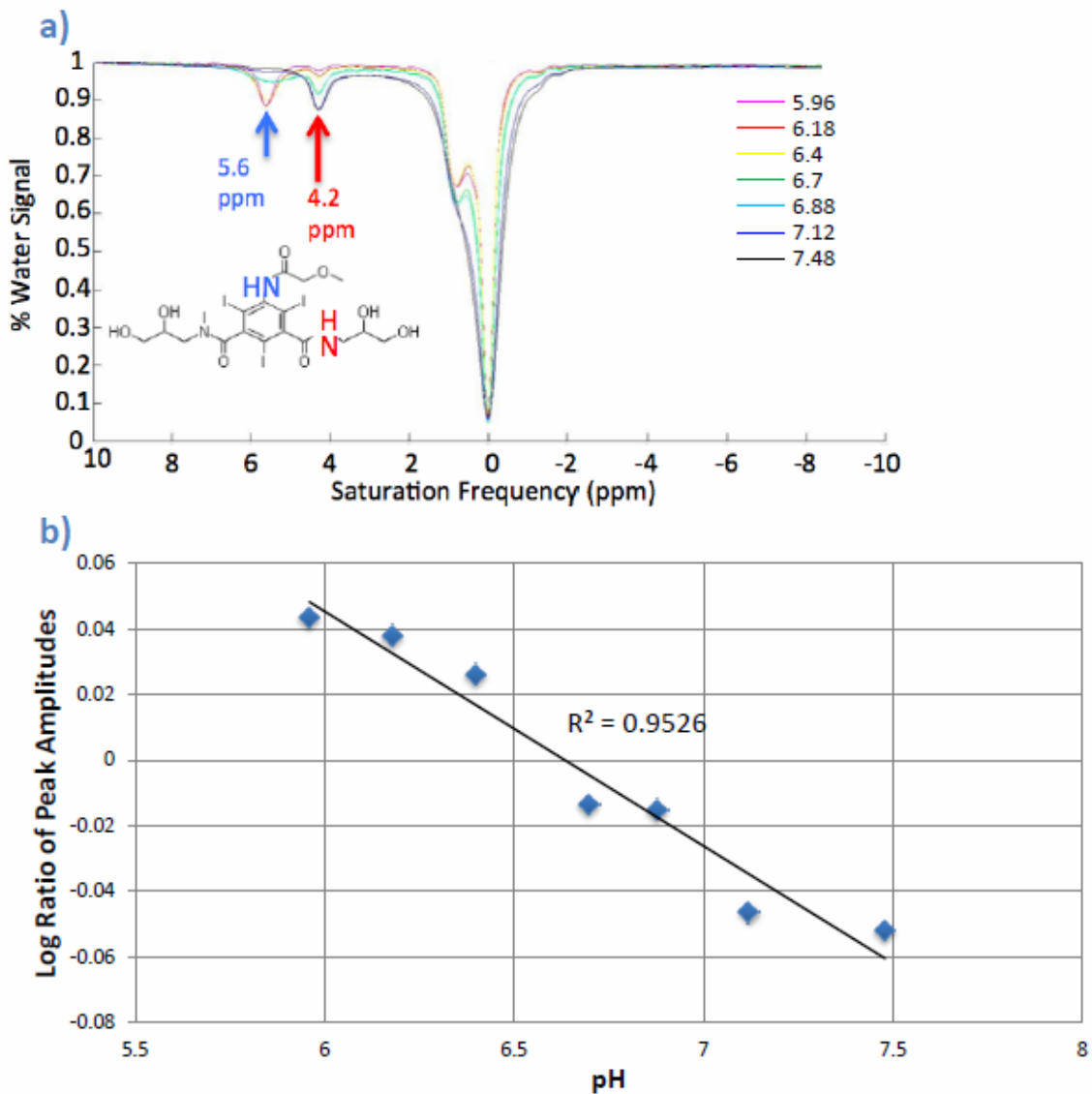

Figure 3: Ultravist® Phantom Results

Z-spectra of Ultravist® phantoms of varying pH (a) with reference image of iopromide structure and amide groups of interest. The log ratio of the 2 peaks corresponding with the amides has a linear regression that correlates with pH with an R^2 of 0.95 (b).

Iopromide (200 mM) was injected into a fresh disc to test its ability to report pH

of the discs using the calibration curve created with the Ultravist® pH phantoms. Figure 4a shows the z-spectra of the Disc+Ultravist® pre- and post- lactate injection. The peaks of the amide groups were visualized in the z-spectra: the amplitude of the peak at 4.2 ppm decreases while the broad peak at 5.6 ppm increases after the addition of lactate to the disc. This result is consistent with the trends from the phantom studies. The ratio of these peaks in the pre- and post-lactate iopromide CEST were 0.93 and 0.96 corresponding with a pH of 7.07 and 6.88 respectively, according to the linear regression equation y = -0.0715x + 0.4744 (Figure 4b).
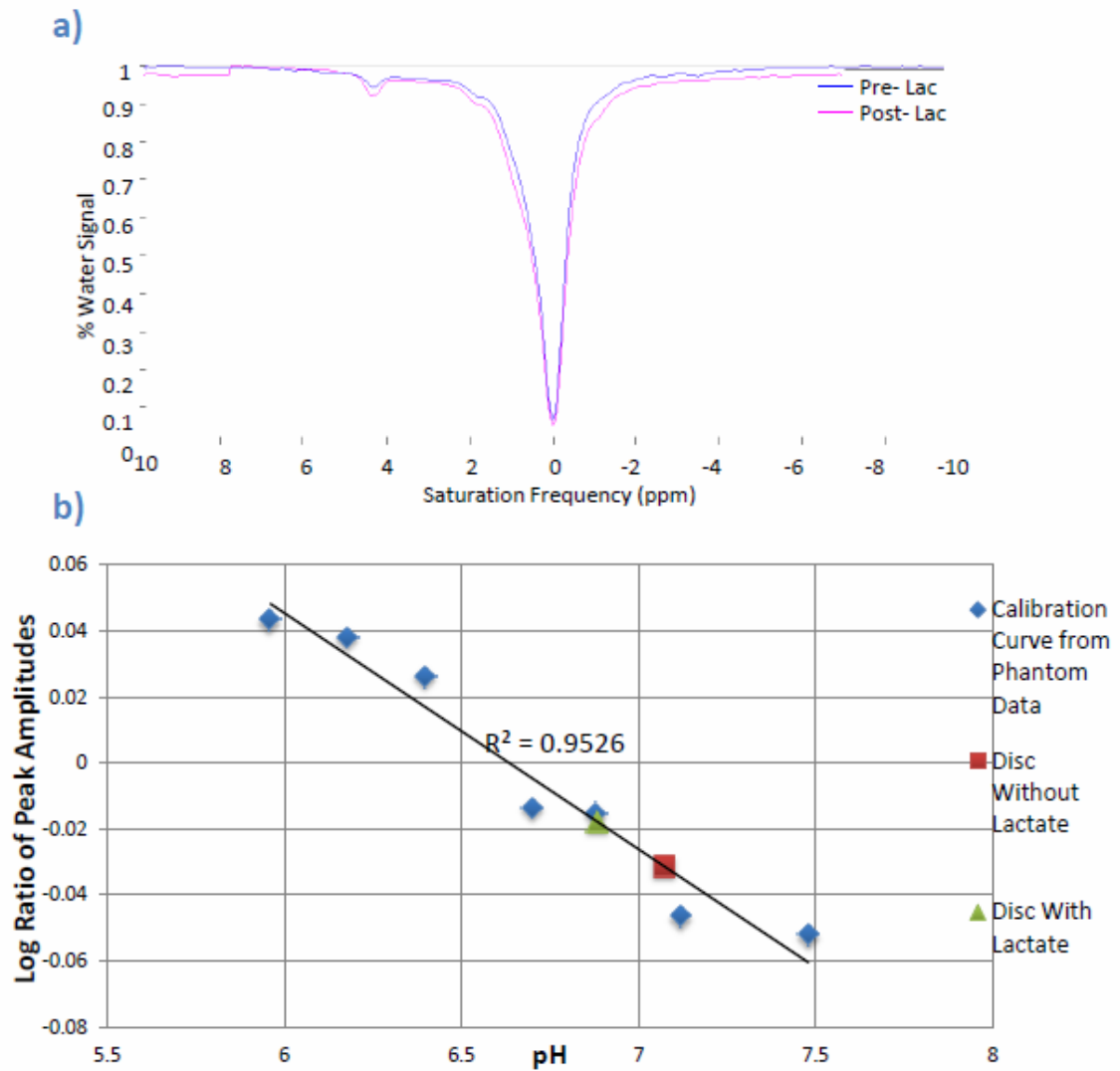
Z-spectra showing changing CEST effect after injection of lactate (shown in blue) (a) and pH of the disc pre- and post-lactate injection as determined using phantom calibration curve (b).

Measuring pH

After imaging studies were completed, the pH of the nucleus pulposus of each of the discs whose pH had been manipulated with lactate (pH = 6.5), as well as 3 in-tact discs to act as controls, were measured using a tissue pH meter and Litmus paper. The pH of the control discs was about 8 and the pH of the discs manipulated with lactate ranged from 7.0 to 7.5. A comparison of the various methods used to measure disc pH is summarized in Table 2.

Type		pH
Lactate Solution	1 M	6.5
Average IVD pH	Literature	7.2 - 7.7
Control Discs	No Lac	8
Discs Manipulated with Lactate	Disc 1	7 - 7.2
	Disc 2	7.3 - 7.5
	Disc 3	7.2 - 7.5
	Disc 4	7.3 - 7.5
	Disc 5	7.3 - 7.5
Discs Measured with Iopromide	Before Lac	7.07
	After Lac	6.88

Table 2: Summary of pH Measurements

Discussion

These findings provide what is to our knowledge the first description of the pH-dependence of gagCEST imaging and the first use of the iopromide contrast agent in the CEST MR imaging of the intervertebral disc specimen. In order to study the changes in gagCEST signal of the disc with changes in pH, we had to somehow manipulate the pH of the nucleus pulposus of the intervertebral disc. The amplitude of the lactate signal was

10 times greater post-lactate, proving that the lactate solution was successfully incorporated into the disc. Average $T_{1\rho}$ values in the disc were calculated and were shown to increase after lactate injection. Because $T_{1\rho}$ is a spin-lattice relaxation that probes interactions between motionally-restricted water molecules and their macromolecular environment, an increase in fluid following the injection of the lactate solution, will cause an increase in $T_{1\rho}$. Lactate and $T_{1\rho}$ imaging were done as checks to ensure that lactate was successfully incorporated into the disc as to manipulate its pH.

The results from the gagCEST studies show the gagCEST asymmetry curves show considerable differences in the CEST effect at varying pH, even if the data from the pH = 6.10 phantom (an outlier) is disregarded. The CEST effect of this phantom is considerably lower than expected. While the reason for this is unclear, one possible explanation for this anomaly is the fact that this experiment was done at 37°C using a heat-pad wrapped around the phantoms. Because the addition of heat changes the rate at which labile protons exchange with bulk water, CEST imaging in general is dependent on temperature. It is possible that the 6.10 phantom was exposed to the heat pad differently than the other phantoms, causing a change the observed CEST phenomenon. Even if the data from this phantom if omitted, however, the results show a non-linear dependency of gagCEST on pH. Using this method to determine the change in disc pH following lactate injection was therefore difficult; this method may not be an effective way to directly measure pH in the disc.

The pH of each disc was measured after all imaging studies were completed. The methods used to report pH posed some problems: first, the tissue pH meter used was designed for larger tissue samples and therefore had difficulty reading the pH of the discs and second, the pH paper only measured pH qualitatively and in increments of 0.5 pH units. The pH of the control discs was slightly higher than the average pH of the

discs *in vivo* reported in the literature, but the pH measurements are consistent with a decrease in pH that we expected to find after injecting an acid directly into the disc.

The Ultravist® pH phantom studies demonstrated a linear change of iopromide CEST with pH in the range of pH = 6 to 7.5, within the expected physiological range. When diluted Ultravist® was injected directly into the disc, the CEST effect was visible and measurable and we were able to report the change in the pH of the disc with the addition of lactate. While the reported pH using iopromide CEST imaging was not consistent with the pH of the disc reported by Litmus paper/tissue pH meter, it was reasonably close to the average pH of a disc *in vivo* as reported in literature [7].

There seems to be a correlation between changes in pH in the disc and discogenic back pain and intervertebral disc degeneration. With further research, this biomarker has the potential to predict surgical outcomes and may one day be used as a tool to refine patient selection for spinal fusion and other surgical procedures [9, 10]. If these relationships are established, measuring pH *in vivo* using non-invasive MRI would be a powerful clinical tool. This study proposes two methods to measure pH in the intervertebral discs. While gagCEST does not seem to vary with pH in a linear way, the ability to measure the ratio of the 2 CEST peaks corresponding with the 2 amide groups in iopromide, a contrast agent already clinically approved and implemented in CT studies, to report pH in the tissue could be valuable in better understanding disease progression and could ultimately be used in surgery or treatment planning.

Conclusions

The mechanisms and progression of intervertebral disc degeneration and its involvement in low back pain are not fully understood. Recent research suggests that certain biochemical changes within the disc, such as a drop in pH as a result of increased

lactate accumulation, not only catalyze disc degeneration, but also serve as markers of pain. While gagCEST has been shown to vary with pH, it is also sensitive to changes in GAG concentration: gagCEST asymmetry decreases with a decrease in GAG concentration [16]. The effect of changing pH and loss of GAG concentration would be difficult to distinguish in *in vivo* experiments; therefore pH of the disc will be difficult to measure using gagCEST. Because iopromide CEST imaging is independent of the local concentration of macromolecules, it shows great potential in reporting pH in intervertebral disc specimen studies. *In vivo* experiments will face the challenge of incorporating the Ultravist® solution into the disc, however. Nevertheless, the ability to non-invasively measure the pH of the intervertebral disc using this method could have significant clinical value in the early prediction of pain and disc degeneration and could therefore help treatment planning and preventative care.

References

(1). Dagenais S, Caro J, Haldeman S. A systemic review of low back pain cost of illness studies in the United States and internationally. Spine. 2008: 8(1); 8-20.

(2). Luoma K, Riihimaki H, Luukkonen R, Raininko R, Viikari-Juntura E, Lamminen A. Low back pain in relation to lumbar disc degeneration. Spine, 2000; 25(4): 487–492.

(3). Adams MA, Roughley PJ. What is intervertebral disc degeneration, and what causes it? Spine, 2006; 31(18): 2151– 2161

(4). Cheung KM. The relationship between disc degeneration, low back pain, and human pain genetics. Spine 2010;10:958-60.

(5). McDevitt CA. In: Ghosh P, ed. Biology of the Intervertebral Disc. Boca Raton, FL: CRC Press; 1988:151-70.

(6). Urban JP. The role of the physicochemical environment in determining disc cell behavior. Biochem So Trans 2002; 30 (Pt 6): 858-64.

(7). Urban JP, Smith S, Fairbank JC. Nutrition of the intervertebral disc. Spine 2004; 29:2700-9.

(8). Bibby SR, Fairbank JC, Urban MR, et al. Metabolism of the intervertebral disc: effects of low levels of oxygen, glucose, and pH on rates of energy metabolism of bovine nucleus pulposus cells. Spine 2005;30:487-96.

(9). Keshari KR, Lotz JC, Link TM, Hu S, Majumdar S, Kurhanewicz J. Lactic acid and proteoglycans as metabolic markers for discogenic back pain. Spine 2008;33(3):312-7.

(10). Liang C, Li H, et al. New hypothesis of chronic back pain: low pH promotes nerve

ingrowth into damaged intervertebral discs. ACTA Anaesthesiologica Scandinavica 2012

(11). Haughton V. Medical Imaging of Intervertebral Disc Degeneration: Current Status of Imaging. Spine 2004; 29(23): 2751-2756.

(12). Finch P. Technology insight: imaging of low back pain. Nat Clin Pract Rheumatol 2006;2:554-61

(13). Terreno E, Castelli DD, Aime S. Encoding the frequency dependence in MRI contrast media: the emerging class of CEST agents. Contrast Media Mol. Imaging 2010; 5: 78–98.

(14). Wolff SD, Balaban RS. Magnetization transfer contrast (MTC) and tissue water proton relaxation in vivo. Magn Reson Med 1989; 10: 135–144.

(15). Ward KM, Aletras AH, Balaban RS. A new class of contrast agents for MRI based on proton chemical exchange dependent saturation transfer (CEST). J Magn Reson 2000; 143: 79–87.

(16). Ling W, Regatte RR, Navon G, Jerschow A. Assessment of glycosaminoglycan concentration in vivo by chemical exchange- dependent saturation transfer (gagCEST). Proc. Natl. Acad. Sci. USA, 2008; 105(7): 2266–2270.)
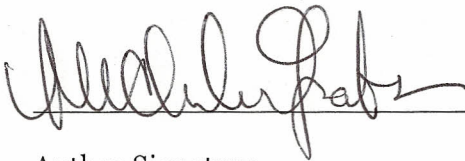
(17). Aime S, Calabi L, Biondi L, De Miranda M, Ghelli S, Paleari L, Rebaudengo C, Terreno E. Iopamidol: exploring the potential use of a well-established X-ray contrast agent for MRI. Magn Reson Med 2005; 53: 830–834.

(18). Liu QC, et al. Measuring extracellular pH within in vivo tumors using a DIACEST MRI contrast agent. Presentation number T115. Scientific Session 11: Imaging probes for novel molecular imaging 2011.

(19). He Q, Shungu DC, van Zijl PC, Bhujwalla ZM, Glickson JD. Single-scan in vivo lactate editing with complete lipid and water suppression by selective multiple-quantum-coherence transfer (Sel-MQC) with application to tumors. J Magn Reson B. 1995;106(3):203-11.

(20). Li X, Han ET, Busse RF, Majumdar S. In vivo T(1rho) mapping in cartilage using 3D magnetization-prepared angle-modulated partitioned k-space spoiled gradient echo snapshots (3D MAPSS). Magn Reson Med. 2008 Feb; 59(2):298-307.

(21). Kim M, Gillen J, Landman BA, Zhou J, van Zijl PC. Water saturation shift referencing (WASSR) for chemical exchange saturation transfer (CEST) experiments. Magn Reson Med 2009; 61: 1441–1450.

Publishing Agreement

It is the policy of the University to encourage the distribution of all theses, dissertations, and manuscripts. Copies of all UCSF theses, dissertations, and manuscripts will be routed to the library via the Graduate Division. The library will make all theses, dissertations, and manuscripts accessible to the public and will preserve these to the best of their abilities, in perpetuity. I hereby grant permission to the Graduate Division of the University of California, San Francisco to release copies of my thesis, dissertation, or manuscript to the Campus Library to provide access and preservation, in whole or in part, in perpetuity.

_____ 09/05/2012
Author Signature   Date